J Neurophysiol
87: 172–182, 2002; 10.1152/jn.00778.2000.

On the Interaction Between Voltage-Gated Conductances and Ca^{2+} Regulation Mechanisms in Retinal Horizontal Cells

YUKI HAYASHIDA AND TETSUYA YAGI
Neurosystems Laboratory, Faculty of Computer Science and Systems Engineering, Kyushu Institute of Technology, Fukuoka 820-8502, Japan

Received 30 October 2000; accepted in final form 14 September 2001

Hayashida, Yuki and Tetsuya Yagi. On the interaction between voltage-gated conductances and Ca^{2+} regulation mechanisms in retinal horizontal cells. *J Neurophysiol* 87: 172–182, 2002; 10.1152/jn.00778.2000. The horizontal cell is a second-order retinal neuron that is depolarized in the dark and responds to light with graded potential changes. In such a nonspiking neuron, not only the voltage-gated ionic conductances but also Ca^{2+} regulation mechanisms, e.g., the Na^+/Ca^{2+} exchange and the Ca^{2+} pump, are considered to play important roles in generating the voltage responses. To elucidate how these physiological mechanisms interact and contribute to generating the responses of the horizontal cell, physiological experiments and computer simulations were made. Fura-2 fluorescence measurements made on dissociated carp horizontal cells showed that intracellular Ca^{2+} concentration ($[Ca^{2+}]_i$) was maintained <100 nM in the resting state and increased with an initial transient to settle at a steady level of $\simeq$600 nM during prolonged applications of L-glutamate (L-glu, 100 μM). A preapplication of caffeine (10 mM) partially suppressed the initial transient of $[Ca^{2+}]_i$ induced by L-glu but did not affect the L-glu-induced steady $[Ca^{2+}]_i$. This suggests that a part of the initial transient can be explained by the Ca^{2+}-induced Ca^{2+} release from the caffeine-sensitive Ca^{2+} store. The Ca^{2+} regulation mechanisms and the ionic conductances found in the horizontal cell were described by model equations and incorporated into a hemi-spherical cable model to simulate the isolated horizontal cell. The physiological ranges of parameters of the model equations describing the voltage-gated conductances, the glutamate-gated conductance and the Na^+/Ca^{2+} exchange were estimated by referring to previous experiments. The parameters of the model equation describing the Ca^{2+} pump were estimated to reproduce the steady levels of $[Ca^{2+}]_i$ measured by Fura-2 fluorescence measurements. Using the cable model with these parameters, we have repeated simulations so that the voltage response and $[Ca^{2+}]_i$ change induced by L-glu applications were reproduced. The simulation study supports the following conclusions. *1*) The Ca^{2+}-dependent inactivation of the voltage-gated Ca^{2+} conductance has a time constant of $\sim$2.86 s. *2*) The falling phase of the $[Ca^{2+}]_i$ transient induced by L-glu is partially due to the inactivation of the voltage-gated Ca^{2+} conductance. *3*) Intracellular Ca^{2+} is extruded mainly by the Na^+/Ca^{2+} exchange when $[Ca^{2+}]_i$ is more than $\sim$2 μM and by the Ca^{2+} pump when $[Ca^{2+}]_i$ is less than $\sim$1 μM. *4*) In the resting state, the Na^+/Ca^{2+} exchange may operate in the reverse mode to induce Ca^{2+} influx and the Ca^{2+} pump extrudes intracellular Ca^{2+} to counteract the influx. The model equations of physiological mechanisms developed in the present study can be used to elucidate the underlying mechanisms of the light-induced response of the horizontal cell in situ.

INTRODUCTION

Neurons generally have resting potentials of around -70 mV and can generate action potentials in response to stimuli. On the other hand, most of the outer retinal neurons of the vertebrate retina are depolarized in the dark and respond to light with graded potential changes. In such neurons, not only the voltage-gated ionic conductances but also the Ca^{2+} regulation mechanisms are thought to play important roles in generating the light-induced responses (Hayashida et al. 1998).

The horizontal cell is a second-order neuron of the vertebrate retina that is tonically depolarized in the dark by an excitatory transmitter, probably L-glutamate, released from the photoreceptors (Cervetto and MacNichol 1972; Dowling and Ripps 1972; Murakami et al. 1972). The membrane properties have been studied in enzymatically dissociated horizontal cells and five types of voltage-gated ionic conductances were identified under the voltage-clamp condition (e.g., Kaneko 1987; Lasater 1991 for reviews; Lasater 1986; Picaud et al. 1998; Shingai and Christensen 1983, 1986; Tachibana 1983; Yagi and Kaneko 1988). Among these voltage-gated conductances, the Ca^{2+}conductance was suggested to play a crucial role in maintaining the membrane potential in the dark (Winslow 1989). More recently, some aspects concerning the Ca^{2+} regulation mechanisms were also revealed in dissociated horizontal cells by the optical measurement using the Ca^{2+}-sensitive dyes (Hayashida et al. 1998; Linn and Christensen 1992; Micci and Christensen 1998; Okada et al. 1999). The Ca^{2+}-regulation mechanisms are thought to affect the horizontal cell response because the voltage-gated Ca^{2+} conductance is known to be inactivated by intracellular Ca^{2+} (Tachibana 1981, 1983). Despite these previous experiments elucidating the electrochemical properties of individual physiological mechanisms, there are few quantitative analyses studying how these ionic conductances and Ca^{2+}-regulation mechanisms interact each other. In the present study, we used a cable model to quantitatively study how the physiological mechanisms identified in in vitro preparations operate together to generate physiological responses of horizontal cells.

Present address and address for reprint requests: T. Yagi, Graduate School of Engineering, Osaka University, Yamada-Oka 2-1, Suita, Osaka 565-0871, Japan (E-mail: yagi@ele.eng.osaka-u.ac.jp).

The costs of publication of this article were defrayed in part by the payment of page charges. The article must therefore be hereby marked "*advertisement*" in accordance with 18 U.S.C. Section 1734 solely to indicate this fact.

METHODS

Physiological experiments

Horizontal cells were dissociated from the retinae of carp, *Cyprinus carpio* (10- to 20-cm body length). The dissociation procedure and the cell preparation appeared in the previous study (Hayashida et al. 1998). The dissociated cells were superfused continuously with a control solution using a "Y"-tube microflow system (Suzuki et al. 1990). The control solution contained (in mM) 120 NaCl, 7.6 KCl, 2.5 $CaCl_2$, 1 $MgCl_2$, 10 glucose, 10 HEPES with 0.1 mg/ml BSA (pH adjusted to 7.3 with 1 M NaOH). A high concentration of K^+ was included in this control solution as was in previous studies on the dissociated cells of the cyprinid fish (Tachibana 1983, 1985; Yagi 1989; Yagi and Kaneko 1988). The general conclusions reached in the present study were not changed when a lower concentration of K^+ (2.6 mM) was used in the control solution (data not shown). For a cobalt application, 1 mM $CaCl_2$ in the control solution was replaced by equimolar $CoCl_2$. For cadmium or caffeine application, 0.2 mM $CdCl_2$ or 10 mM caffeine was added to the control solution. Ca^{2+}-free solution was made by removing $CaCl_2$ from the control solution and, in some cases, adding 5 mM EGTA. When L-glutamate was applied to the cell, sodium L-glutamate (100 μM) was dissolved in superfusates. Pharmacological agents were applied using the "Y"-tube microflow system, whose outlet (internal tip diameter, ~500 μm) was located within ~500 μm from the recorded cell.

$[Ca^{2+}]_i$ was ratiometrically measured by using the fluorescent Ca^{2+} indicator, Fura-2 (Grynkiewicz et al. 1985). Fura-2 fluorescence measurements from dissociated horizontal cells have been described in a previous study (Hayashida et al. 1998). In brief, the isolated cells were incubated in Fura-2/AM solution in the dark for 30–40 min at room temperature. The Fura-2/AM solution was made by adding the membrane-permeant analogue Fura-2 acetoxymethyl ester (Fura-2/AM) to the control solution to a final concentration of 5 μM (<0.1% vol/vol DMSO). The cells were then rinsed twice with control solution and maintained in culture medium for >30 min to convert Fura-2/AM to the Ca^{2+}-sensitive form.

The 340- and 380-nm excitation light was used and the fluorescence emitted by cells was measured at 510 nm. The ratio of the fluorescence intensities elicited with the 340- and 380-nm excitation light was calculated after subtracting the background fluorescence. $[Ca^{2+}]_i$ was calculated from the fluorescence ratio (R) according to the following formula of Grynkiewicz et al. (1985)

$$[Ca^{2+}]_i = K_d \cdot (F_{free}/F_{bound}) \cdot (R - R_{min})/(R_{max} - R) \quad (1)$$

Here K_d is the equilibrium dissociation constant for Fura-2 at 20°C (135 nM) (Grynkiewicz et al. 1985). In the present study, R_{min} was estimated as the ratio obtained when a cell was superfused with a Ca^{2+} ionophore, 4-Br-A23187 or A23187 (10 μM), in a Ca^{2+}-free solution (10 mM EGTA and no Ca^{2+} added). The R_{max} value was determined as the ratio when a cell was superfused with the Ca^{2+} ionophore in a high-Ca^{2+} solution (5 mM Ca^{2+}). F_{free} and F_{bound} were determined as the fluorescence intensities at 380-nm excitation when a cell was superfused with the Ca^{2+} ionophore in the Ca^{2+}-free solution and the high-Ca^{2+} solution, respectively. In the text, $[Ca^{2+}]_i$ values are given when the values of F_{free}, F_{bound}, R_{min}, and R_{max} were obtained for each cell at the end of the recording. Otherwise, only the R values are given (denoted as "fluorescence ratio" in the relevant text figures).

In the voltage- and current-clamp experiments, the perforated-patch technique with the whole cell configuration was employed to minimize disruption of cytoplasmic constituents (Horn and Marty 1988).

Computer simulations

Computer simulations were carried out using the simulation software NEURON (Hines and Carnevale 1997).

Since we preferentially used horizontal cells which have round-shaped somata and a few short thin dendrites in the present experiments, a hemi-spherical cable is considered to be appropriate for modeling the dissociated horizontal cell. As shown in Fig. 1, a dissociated horizontal cell was modeled by a hemi-spherical cable with 15 μm of radius. This cable dimension mimicked a typical shape of the dissociated horizontal cells used in the present experiments. The simulation was conducted with a single cylindrical cable model as well. The diameter and length of the cable were 20 and 22.5 μm, respectively. The internal volume and surface area of the cable are the same as those of the hemi-spherical cable. There is no distinguishable difference in simulation results between these two models. Therefore only the simulation results obtained with the hemi-spherical cable are described in this paper.

In the simulations, intracellular Ca^{2+} diffusion in the longitudinal direction was taken into account by dividing the cable into 202 segments (Hines and Carnevale 2000). Intracellular Ca^{2+} diffusion in the radial direction was also taken into account by dividing the each segment into 101 shells. The diffusion between neighboring shells is described by (Hines and Carnevale 2000)

$$[Ca^{2+}]_j \xleftrightarrow{D_{Ca} \cdot a_{j,j+1}/d_{j,j+1}} [Ca^{2+}]_{j+1}$$

Here, j is an integer from 0 to 100 representing the shell number; $[Ca^{2+}]_j$ is the Ca^{2+} concentration in the shell of j, e.g., $j = 0$ for the outer most shell; $a_{j,j+1}$ and $d_{j,j+1}$ are the area of the border and the distance between the shells of j and $j + 1$; D_{Ca} is the diffusion constant for intracellular Ca^{2+} (units of $\mu m^2/s$). D_{Ca} used in the present simulations was assumed to be 6 $\mu m^2/s$ and is in the range of the apparent diffusion constant of Ca^{2+} measured in a living cell (Kushmerick and Podolsky 1969).

The number of segments and shells were increased in the simulation to estimate the error of the calculation.

A step of calculation time was 20–50 μs in all simulations.

RESULTS

Physiological experiments

$[Ca^{2+}]_i$ CHANGE INDUCED BY L-GLU. Figure 2*A* shows an example of the $[Ca^{2+}]_i$ change in response to a prolonged application of L-glu (100 μM) to an isolated horizontal cell. In this experiment, the cell was first superfused with the control solution to measure $[Ca^{2+}]_i$ in the resting state. The resting potential of the isolated horizontal cell was more negative than

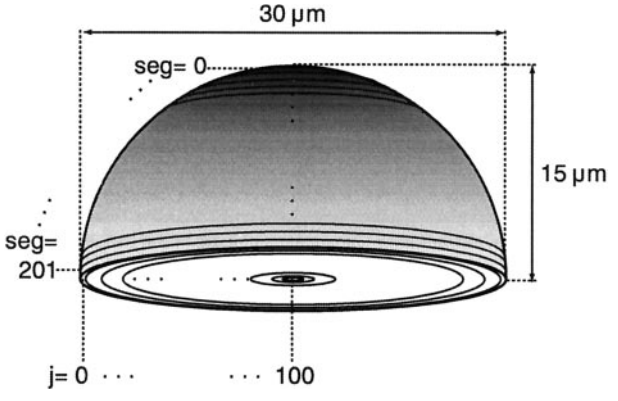

FIG. 1. A hemi-spherical cable model for a dissociated horizontal cell. Radius of the cable is 15 μm. The cable is divided into 202 segments in the longitudinal direction, as indicated by seg. Internal space of each segment is divided into 101 shells in the radial direction, as indicated by j (see text for detail).

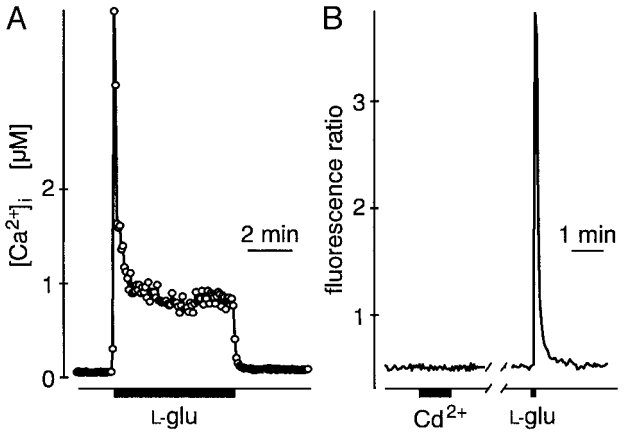

FIG. 2. $[Ca^{2+}]_i$ change measured in the isolated horizontal cell. *A*: 100 μM L-glutamate was applied for 324 s. The fluorescence ratio of Fura-2 was measured every 4 s (○). $[Ca^{2+}]_i$ was calculated by measuring the calibration parameters for this cell at the end of this recording (METHODS). *B*: 200 μM Cd^{2+} was applied for 60 s and then 100 μM L-glutamate was applied for 9 s. *A* and *B* were obtained in different cells. The membrane potential was not clamped and was not recorded both in *A* and *B*.

−50 mV in the control solution [−56.2 ± 6.0 (SD) mV, n = 5] (Hayashida et al. 1998; Tachibana 1981). At this voltage, voltage-gated Ca^{2+} current was not detectable by the voltage-clamp experiments (Tachibana 1983; Yagi and Kaneko 1988). $[Ca^{2+}]_i$ in the resting state was ~52 nM in this cell [75 ± 37 (SD) nM, n = 11]. The resting $[Ca^{2+}]_i$ was not affected by 200 μM Cd^{2+} (n = 5) as shown in Fig. 2*B*. Furthermore, application of 1 mM Co^{2+} did not have effects on $[Ca^{2+}]_i$ in the resting state (n = 4, data not shown). These observations confirm the results obtained by the voltage-clamp experiments.

During the L-glu application, $[Ca^{2+}]_i$ transiently increased to the maximum level and then gradually decreased to reach a steady level of ~0.82 μM (0.59 ± 0.23 μM, n = 11). $[Ca^{2+}]_i$ changed little when L-glu (100 μM) was applied to the cell in the Ca^{2+}-free solution (n = 6, data not shown). Ca^{2+} is known to enter the horizontal cell through the glutamate-gated cation conductance (Hayashida et al. 1998; Linn and Christensen 1992; Okada et al. 1999) as well as the voltage-gated Ca^{2+} conductance. The relative amount of Ca^{2+} entering the isolated cell through these conductances was examined by a voltage-clamp experiment shown in Fig. 3, *A* and *B*. We first measured a change of $[Ca^{2+}]_i$ induced by L-glu (100 μM) when the membrane voltage was clamped at −75 mV (Fig. 3*A*). As shown in the figure, $[Ca^{2+}]_i$ was slightly increased by the L-glu application (indicated by a). This increase of $[Ca^{2+}]_i$ is due to the Ca^{2+} influx through the glutamate-gated conductance because the voltage-gated Ca^{2+} conductance was not activated at this voltage. The increase of $[Ca^{2+}]_i$, however, was much smaller than that induced by the depolarization of membrane to −10 mV (b). Similar results were obtained for eight of nine cells examined. The membrane potential of the isolated horizontal cell was maintained at approximately −5 mV during the application of 100 μM L-glu (Hayashida et al. 1998). When the membrane potential was clamped to −5 from −55 mV, $[Ca^{2+}]_i$ transiently increased and then gradually decreased to reach a steady level (Fig. 3*B*, b). At this steady level, L-glu (100 μM) application induced a sustained inward current but only a small increase of $[Ca^{2+}]_i$ was seen (indicated by a). Similar results were obtained for seven of eight cells examined. These observations suggest that the Ca^{2+} influx occurs mainly through the voltage-gated Ca^{2+} conductance during applications of 100 μM L-glu to isolated horizontal cell.

INITIAL TRANSIENT OF $[Ca^{2+}]_i$ INDUCED BY L-GLU. The transient increase of $[Ca^{2+}]_i$ shown in Fig. 2*A* was suppressed by a preapplication of caffeine (Fig. 4). L-Glu (100 μM) was applied to the cell repetitively as shown in the figure. In the second trial, 10 mM caffeine was applied immediately before the application of L-glu. $[Ca^{2+}]_i$ transiently increased and then decreased toward the resting level in response to the caffeine application (see *inset*). The transient increase of $[Ca^{2+}]_i$ induced by L-glu was partially suppressed to ~60% (61 ± 26%, mean ± SD, n = 7) when the caffeine was preapplied in seven of nine cells examined. In the remaining two cells, the initial transient was completely suppressed (Fig. 4*B*). The transient increase of $[Ca^{2+}]_i$ recovered in the third trial (*A* and *B*). The suppression of the transient increase of $[Ca^{2+}]_i$ by caffeine is likely to be due to a prolonged depletion of Ca^{2+} store. This observation suggests that a part of the initial transient of $[Ca^{2+}]_i$ can be explained by the Ca^{2+}-induced Ca^{2+} release (CICR) from the caffeine-sensitive Ca^{2+} store (DISCUSSION).

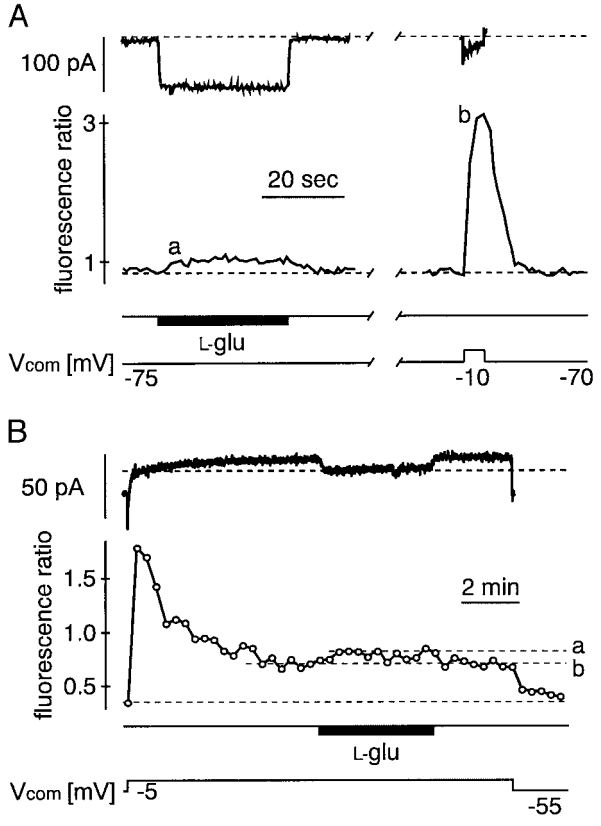

FIG. 3. Relative contribution of the voltage-gated Ca^{2+} conductance and the glutamate-gated conductance to the L-glu-induced $[Ca^{2+}]_i$ change. *A*: L-glutamate (100 μM) was applied for 32 s during the voltage clamp in the perforated-patch configuration. The holding voltage was −75 mV (*bottom*) and then the membrane voltage was depolarized to −10 mV for 5 s. The whole cell membrane current (*top*) and the Fura-2 fluorescence ratio (*middle*) were simultaneously measured. ···, the 0 pA level in the current trace. The fluorescence ratio was measured once every second. *B*: the holding voltage was −55 mV (*bottom*) and then the membrane voltage was depolarized to −5 mV for 800 s. L-Glutamate (100 μM) was applied for 240 s during the membrane potential was clamped at −5 mV. The whole cell membrane current (*top*) and the Fura-2 fluorescence ratio (*middle*) were simultaneously measured. ···, the 0 pA level in the current trace. The fluorescence ratio was measured every 20 s.

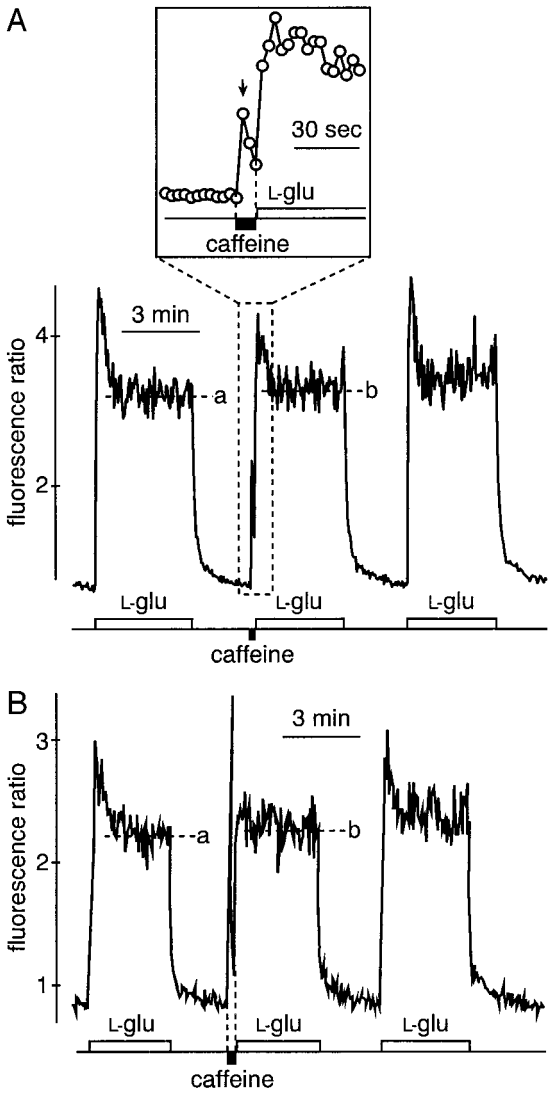

FIG. 4. Initial transient of $[Ca^{2+}]_i$ change. L-Glutamate (100 μM) was applied repetitively for ~3 min with 2-min intervals. In the second trial, 10 mM caffeine was preapplied for ~10–20 s immediately before the L-glu application. The Fura-2 fluorescence ratio was measured every 3 s. The membrane potential was not clamped and was not recorded. *A*: partial suppression of the initial transient by the caffeine preapplication. The caffeine-induced Ca^{2+} release was shown in the inset with an expanded time scale. *B*: complete blockade of the initial transient by the caffeine preapplication.

The remaining component of the initial transient, which was not blocked by the preapplication of caffeine (Fig. 4*A*), is explained by the Ca^{2+}-dependent inactivation of the voltage-gated Ca^{2+} conductance, which will be shown later with quantitative analyses using the biophysical model of the isolated horizontal cell.

In contrast to the initial transient, the steady levels of $[Ca^{2+}]_i$ during the prolonged L-glu application were not affected by the preapplication of caffeine (indicated by a and b).

Biophysical model of the isolated horizontal cell

MODELS OF PHYSIOLOGICAL MECHANISMS. The physiological mechanisms relevant to calculate $[Ca^{2+}]_i$ were the glutamate-gated cation conductance, the voltage-gated Ca^{2+} conductance, the Na^+/Ca^{2+} exchange, the Ca^{2+} pump, and Ca^{2+} buffering. These mechanisms were described by the following equations.

Ca^{2+} influx through the glutamate-gated cation conductance has been reported in fish horizontal cells (Hayashida et al. 1998; Linn and Christensen 1992; Okada et al. 1999). Within the range of membrane potential considered in the present study (−60 to 0 mV), the cation current through the glutamate-gated conductance depends on the membrane potential almost linearly (Tachibana 1985). Thus the glutamate-gated cation current was described by an equation

$$I_{glu} = g_{glu}(t) \cdot (V_m - E_{glu}) \quad (2)$$

Here, V_m is the membrane potential; E_{glu} is the reversal potential of the cation current that is ~0 mV (Ishida and Neyton 1985; Ishida et al. 1984; Murakami and Takahashi 1987; Tachibana 1985); $g_{glu}(t)$ is the glutamate-gated conductance (units of mS/cm^2). The *N*-methyl-D-aspartate (NMDA)-type glutamate receptor has been found in the catfish horizontal cell (O'Dell and Christensen 1986, 1989), but not in the horizontal cell of cyprinid fish (Ishida et al. 1984; Lasater and Dowling 1982). The spatial distribution of the glutamate receptors over the dissociated horizontal cell membrane is thought to be almost homogeneous (Ishida et al. 1984). Therefore the glutamate-gated cation conductance expressed by *Eq. 2* was distributed homogeneously over the entire lateral surface of the cable shown in Fig. 1. To simulate the response to a L-glu application, $g_{glu}(t)$ was modulated with an equation

$$g_{glu}(t) = \begin{cases} 0 & \text{for } t \le t_{on} \\ \overline{g_{glu}} \cdot \{1 - \exp(-(t - t_{on})/\tau_{glu})\} & \text{for } t_{on} < t \le t_{off} \\ \overline{g_{glu}} \cdot \{1 - \exp(-(t_{off} - t_{on})/\tau_{glu})\} \cdot \{\exp(-(t - t_{off})/\tau_{glu})\} & \text{for } t > t_{off} \end{cases} \quad (3)$$

Here, $\overline{g_{glu}}$ is the maximum conductance activated by the application of 100 μM L-glu; L-glu is applied at t_{on} and removed at t_{off}; τ_{glu} reflects two time constants, the activation time constant of glutamate channels and the time constant of glutamate increase by the "Y"-tube microflow system (METHODS). Because the activation time constant of the channels is expected to be much faster than the time constant of glutamate increase by the "Y"-tube system, τ_{glu} is considered to mainly represent the time constant of glutamate increase. $\overline{g_{glu}}$ was estimated from the data obtained by Tachibana (1985). τ_{glu} was selected to be 100 ms to simulate the time course of activation of the glutamate-gated current induced by L-glu applications with the present method. The ratio of the current carried by Ca^{2+} to I_{glu} through the glutamate-gated conductance was assumed to be 1% and is in the range of the fractional Ca^{2+} current through AMPA-receptor channels (Jonas and Burnashev 1995).

The high-threshold and sustained voltage-gated Ca^{2+} conductance was found in the isolated goldfish horizontal cell (Tachibana 1983; Yagi and Kaneko 1988). A transient type of Ca^{2+} conductance has been identified in the horizontal cells of white bass (Sullivan and Lasater 1992) but not in the horizontal cell of cyprinid fish. Therefore Ca^{2+} current through the volt-

TABLE 1. *Parameter values of the model equations for the Ca^{2+}-related physiological mechanisms*

Physiological Mechanisms	Estimated Values	Units
Intracellular Ca^{2+} diffusion	$D_{Ca} = 6$	[$\mu m^2/s$]
Glutamate-gated cation conductance	$E_{glu} = 0$	[mV]
	$\overline{g_{glu}} = 232$	[$\mu S/cm^2$]
	$\overline{\tau_{glu}} = 100$	[ms]
Voltage-gated Ca^{2+} conductance	$g_{Ca} = 120$	[$\mu S/cm^2$]
	$\alpha_{m_{Ca}} = 33 \cdot \frac{92.7 - V_m}{\exp((92.7-V_m)/9.6)-1}$	[1/ms]
	$\beta_{m_{Ca}} = 3.3 \cdot \exp((-65.2 - V_m)/11.25)$	[1/ms]
	$K_{Ca} = 0.3$	[μM]
	$n_{Ca} = 4$	
	$\tau_{Ca} = 2.86$	[s]
Na^+/Ca^{2+} exchange	$k_{ex} = 60$	[$pA/cm^2/mM^4$]
	$[Na^+]_i = 8$	[mM]
	$[Ca^{2+}]_{out} = 2.5$	[mM]
	$[Na^+]_{out} = 120$	[mM]
	$n = 3$	
	$r = 0.59$	
Ca^{2+} pump	$A_{pump} = 1.3$	[$pmol/s/cm^2$]
	$K_{pump} = 0.4$	[μM]
Ca^{2+} buffer	$f = 19$	[1/μM/s]
	$b = 0.95$	[1/s]
	$[Buffer]_{total} = 5$	[μM]

See text for details.

age-gated Ca^{2+} conductance in the present case was described by

$$I_{Ca} = \overline{g_{Ca}} \cdot m_{Ca} \cdot h_{Ca} \cdot (V_m - E_{Ca}) \quad (4)$$

$$\frac{dm_{Ca}}{dt} = \alpha_{m_{Ca}} \cdot (1 - m_{Ca}) - \beta_{m_{Ca}} \cdot m_{Ca}$$

$$h_{Ca} + \tau_{Ca} \frac{dh_{Ca}}{dt} = K_{Ca}^{n_{Ca}} / (K_{Ca}^{n_{Ca}} + [Ca^{2+}]_{j=0}^{n_{Ca}}) \quad (5)$$

Here, E_{Ca} is the reversal potential of Ca^{2+}; g_{Ca} is the maximum conductance (units of $\mu S/cm^2$); m_{Ca} and h_{Ca} are the activation and the inactivation variables, respectively. α_{mCa} and β_{mCa} are forward and backward rate coefficients, respectively (units of 1/ms) and are functions of the membrane potential as shown in Table 1. The inactivation variable is known to be dependent on intracellular Ca^{2+} (Tachibana 1981, 1983) and was expressed as a function of $[Ca^{2+}]_{j=0}$, which is the Ca^{2+} concentration in the shell just below the membrane. In a steady state in which $dh_{Ca}/dt = 0$, the conductance is half inactivated when $[Ca^{2+}]_i$ is equal to K_{Ca}. n_{Ca} is the Hill coefficient. α_{mCa}, β_{mCa} and $\overline{g_{Ca}}$ were selected to fit the voltage-dependent properties of the conductance obtained by Tachibana (1983). K_{Ca} and n_{Ca} of *Eq. 5* were evaluated from the following observations.

In Fig. 5, the inactivation curve in the steady state was plotted as a function of $[Ca^{2+}]_i$ with different K_{Ca} and n_{Ca}. As shown in the figure, the inactivation curve shifts along the horizontal axis with K_{Ca} (a, c, and e) and the slope of curve changes with n_{Ca} (b, c, and d). As was shown in the previous section, $[Ca^{2+}]_i$ of the isolated horizontal cell was ~75 nM in the resting state. We assumed that 98% of the conductance was not inactivated at this resting $[Ca^{2+}]_i$ (indicated by rest). In the L-glu-induced sustained depolarization, on the other hand, $[Ca^{2+}]_i$ was ~0.59 μM and a few picoamps of inward Ca^{2+} current remained (Hayashida et al. 1998). The Ca^{2+} current is ~100 pA before the inactivation at this voltage (Tachibana 1983), and therefore ~95% of the conductance was thought to be inactivated in this state (indicated by depo). For the steady state inactivation curve described by *Eq. 5* to meet these conditions, n_{Ca} needs to be larger than 4 and K_{Ca} is found to be ~300 nM. Accordingly, n_{Ca} was taken to be 4 because it is consistent with recent observations (Ehlers and Augustine 1999).

It has been reported in the bipolar cell that the inactivation process has a slow time constant (2–5 s) (vonGersdorff and Matthews 1996). The Ca^{2+} current of isolated horizontal cells also inactivates with a slow time course (see Fig. 3*A* of Tachibana 1983). Therefore the time constant τ_{Ca} was introduced in *Eq. 5*. The time course of the Ca^{2+}-dependent inactivation in the horizontal cell will be elucidated to estimate τ_{Ca} later.

The Na^+/Ca^{2+} exchange current of the isolated horizontal

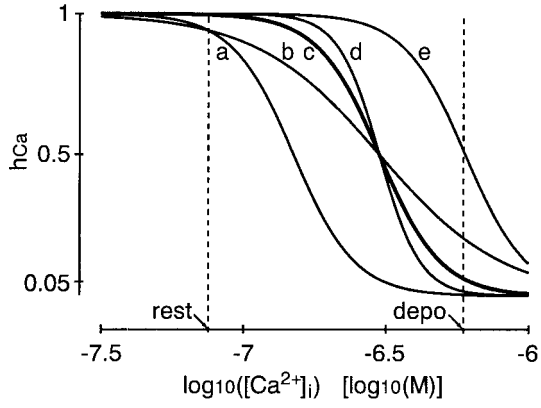

FIG. 5. Inactivation curve of the voltage-gated Ca^{2+} conductance with different values of K_{Ca} and n_{Ca}. a, c, and e illustrate the curve with K_{Ca} = 150, 300, and 600 nM, respectively (n_{Ca} = 4). b, c, and d indicate the curve with n_{Ca} = 2, 4, and 6, respectively (K_{Ca} = 300 nM). rest and depo indicate the $[Ca^{2+}]_i$ in the resting state and in the L-glu-induced sustained depolarization, respectively.

cell was found to fit the following equation (Hayashida et al. 1998)

$$I_{ex} = k_{ex}\{[Na^+]_i^n[Ca^{2+}]_{out}\exp((n-2)rV_mF/R/T) - [Na^+]_{out}^n[Ca^{2+}]_{j=0}\exp(-(n-2)(1-r)V_mF/R/T)\} \quad (6)$$

Here, k_{ex} is a scaling coefficient (units of $pA/cm^2/mM^4$), which is relevant to a density of exchanger molecules in the membrane; $[Na^+]_i$ and $[Na^+]_{out}$ are concentrations of Na^+ inside and outside the cell, respectively; $[Ca^{2+}]_{out}$ is the extracellular Ca^{2+} concentration; n is the stoichiometry for Na^+ and Ca^{2+}; r is related to the position of an energy barrier in the plasma membrane defined by the rate-theory; F, R, and T are the Faraday constant, the gas constant and the absolute temperature, respectively. The values of k_{ex}, n, and r of *Eq. 6* were estimated to be 60 $pA/cm^2/mM^4$, 3 and 0.59, respectively (Hayashida et al. 1998). $[Na^+]_{out}$ and $[Ca^{2+}]_{out}$ correspond to the concentrations of the bath solution used in the experiment. In rod outer segments, K^+ is co-transported with Ca^{2+} by the Na^+/Ca^{2+}, K^+ exchange and a stoichiometry for Na^+ is 4 (Cervetto et al. 1989). However, K^+ dependency of the Na^+/Ca^{2+} exchange was not found in the horizontal cell (Hayashida et al. 1998). Therefore the ratio of exchange was assumed to be Na^+:Ca^{2+} = 3:1 and therefore the current carried by Ca^{2+} is equal to $-2 \times I_{ex}$.

The Ca^{2+} efflux by the Ca^{2+} pump was described by (Zador et al. 1990)

$$flux_{pump} = A_{pump} \cdot [Ca^{2+}]_{j=0}/(K_{pump} + [Ca^{2+}]_{j=0}) \quad (7)$$

Here, $flux_{pump}$ is an amount of Ca^{2+} efflux (units of $pmol/cm^2/s$); A_{pump} is the maximum pumping rate (units of $pmol/cm^2/s$); K_{pump} is the dissociation constant. In the present study, the current carried by Ca^{2+} pump was not taken into account, for simplicity.

Ca^{2+} regulation by a Ca^{2+} buffer was described by a single binding site model

$$[Ca^{2+}]_j + [Buffer]_j \underset{b}{\overset{f}{\rightleftharpoons}} [CaBuffer]_j$$

$$[CaBuffer]_{total} = [Buffer] + [CaBuffer],\ K_{buf} = b/f \quad (8)$$

Here, $[Buffer]_j$ and $[CaBuffer]_j$ are concentrations of the free buffer and the buffer binding Ca^{2+}, respectively; f and b are the rates of the binding and unbinding reactions, respectively (units of $\mu M^{-1}s^{-1}$ for f and s^{-1} for b). In the present study, the values of f and b were assumed to be 19 $\mu M^{-1}s^{-1}$ and 0.95 s^{-1}, respectively (Lee et al. 2000).

The Ca^{2+} store was not taken into account in the present simulation (DISCUSSION).

To calculate the membrane potential of the isolated cell, the voltage-gated K^+ conductances found in the goldfish horizontal cell, i.e., the anomalous rectifier, the delayed rectifier and the transient A-type conductances were also taken into account (Tachibana 1983). Each of these voltage-gated K^+ currents were described by equations

$$I_x = \overline{g_x} \cdot m_x^{p_x} \cdot h_x^{q_x} \cdot (V_m - E_K)$$

$$\frac{dm_x}{dt} = \alpha_{m_x} \cdot (1 - m_x) - \beta_{m_x} \cdot m_x$$

$$\frac{dh_x}{dt} = \alpha_{h_x} \cdot (1 - h_x) - \beta_{h_x} \cdot h_x \quad (9)$$

Here, $\overline{g_x}$ is the maximum conductance (units of $\mu S/cm^2$); m_x and h_x are the activation and inactivation variables, respectively; p_x and q_x are integers; E_K is the reversal potential of K^+. α_{mx} (α_{hx}) and β_{mx} (β_{hx}) are forward and backward rate constants, respectively (units of 1/ms). These are functions of the membrane potential and expressed by the equations shown in Table 2. The parameters included in preceding equations were estimated to fit previous experiments (Tachibana 1983) and are shown in Table 2.

To construct a biophysical model of the isolated horizontal cell, the physiological mechanisms explained above were incorporated into the cable shown in Fig. 1. All the physiological mechanisms expressed by *Eqs. 2–9* except for *Eq. 8* (Ca^{2+} buffer) were incorporated into the lateral surface of the cable (Fig. 1, indicated by shadow). These mechanisms were not included in the bottom and the top surface at the ends of the cable. The passive leakage conductance and the membrane capacitance (Yagi 1989) were also incorporated in the lateral but not in the bottom and top surfaces of the cable. The Ca^{2+} buffer was distributed evenly in the internal space of the cable. Diffusion of the Ca^{2+} buffer was neglected in the present simulations.

The physiological mechanisms, i.e., the glutamate-gated conductance, the voltage-gated ionic conductances, the Ca^{2+} efflux mechanisms, the passive leakage conductance and the membrane capacitance were assumed to distribute homogeneously over the entire lateral surface of the cable.

Estimation of parameter values of Ca^{2+} pump

To conduct physiologically plausible simulations, values of the parameters in the model equations describing the physiological mechanisms require appropriate estimation. As was explained in the previous section, some parameters can be directly estimated referring to previous experiments. We used the following logic to estimate parameter values that cannot be explicitly found from previous experiments. Steady state was assumed in the resting state as well as the prolonged application of L-glu for all physiological mechanisms. All cytoplasmic Ca^{2+} sequestration sites, i.e., Ca^{2+}buffers and Ca^{2+} stores were also at steady state (no net release or storing of Ca^{2+} taking place). Therefore the efflux of Ca^{2+} by the Na^+/Ca^{2+} exchange and the Ca^{2+} pump counterbalances the influx through the glutamate-gated cation and the voltage-gated Ca^{2+} conductances both in the resting state and in the L-glu-induced depolarization. Figure 6 illustrates how such steady states were achieved in the horizontal cell. The efflux of Ca^{2+} by each Ca^{2+} regulation mechanism was plotted as a function of $[Ca^{2+}]_i$ for the resting (*A*) and the L-glu-induced depolarized states (*B*). The total flux was plotted with a thick line (indicated by net). $[Ca^{2+}]_i$ in each steady state corresponds to a point where there is no net flux. The Ca^{2+} flux induced by the Na^+/Ca^{2+} exchange (NaCa) becomes inward when $[Ca^{2+}]_i$ decreases below a value at which the electrochemical gradient reverses. Based on previous experiments, the parameters included in the glutamate-gated cation conductance, the voltage-gated Ca^{2+} conductance and the Na^+/Ca^{2+} exchange were estimated. We selected parameter values for the Ca^{2+} pump, i.e., A_{pump} and K_{pump} of *Eq. 7*, so that the $[Ca^{2+}]_i$ was reproduced in the resting state (~52 nM) as well as in the prolonged

L-glu application (~818 nM). The estimated values were 1.3 pmol/cm^2/s for A_{pump} and 400 nM for K_{pump}.

Inactivation of Ca^{2+} current

The time course of the Ca^{2+}-dependent inactivation observed in the isolated horizontal cell was analyzed by the model to estimate τ_{Ca} of *Eq. 5*. The inactivation time course of voltage-gated Ca^{2+} current during the voltage clamp was calculated with different values of τ_{Ca} using the model as shown in Fig. 7. The model includes the voltage-gated Ca^{2+} conductance, the Na^+/Ca^{2+} exchange, the Ca^{2+} pump, the Ca^{2+} buffer, and the Ca^{2+} diffusion, and therefore the simulation mimics satisfactorily the physiological experiments conducted on the isolated horizontal cell. The experimental data (○) were replotted from Fig. 6 of Tachibana (1983), in which the membrane currents were measured in the isolated goldfish horizontal cell with the micro electrode. All the voltage-gated K^+ currents were blocked and the current induced by clamping the voltage from −61 to 0 mV was measured in the absence (indicated by exp:control) and the presence of 4 mM Co^{2+} (indicated by exp:Co^{2+}). The calculated current illustrates the Co^{2+}-sensitive current that is composed of those through the voltage-gated Ca^{2+} conductance and the Na^+/Ca^{2+} exchange. The calculated current decayed much faster than experimental data when τ_{Ca} was removed (indicated by a and *middle trace* in the *inset*). $[Ca^{2+}]_{j=0}$, the Ca^{2+} concentration just below the membrane, increases quickly after the activation of voltage-gated Ca^{2+} conductance by the depolarization (*bottom trace* in the *inset*) and immediately inactivates the conductance if τ_{Ca} were negligibly small. The time course of calculated current provided a reasonable fit to the experimental data (indicated by b), when τ_{Ca} is 2.86 s. The experimental data could not be fitted by changing the diffusion constant of intracellular Ca^{2+}.

Simulation of L-glu-induced $[Ca^{2+}]_i$ change

Using the parameter values estimated in the previous sections, we simulated the experiments shown in Fig. 2*A*. The densities of each physiological mechanism in the cell model, i.e., g_{glu}, g_{Ca}, k_{ex}, A_{pump}, $[Buffer]_{total}$, and D_{Ca} were adjusted to reproduce the profile of Fig. 2*A*. Fig. 8*A* shows the L-glu-induced $[Ca^{2+}]_i$ change calculated with the cell model (—). Note that the cell model includes all the membrane conductances, the membrane capacitance, and the Ca^{2+}-related physiological mechanisms introduced in the present study. In this figure, the average concentration of intracellular Ca^{2+} of the cable was illustrated to be compared with the Fura-2 fluorescence measurement. The profile of $[Ca^{2+}]_i$ change calculated with the cell model provides an appropriate fit to the experimental data (○) except for the initial transient. The initial transient of $[Ca^{2+}]_i$ estimated by the experiment, however, exceeded the measurable range of Fura-2 (higher than a few μM) (Grynkiewicz et al. 1985) and is likely to include a large error. The discrepancy between the experiment and the simulation probably reflects the error of the Fura-2 fluorescence measurement in such high $[Ca^{2+}]_i$. Another possibility to explain the discrepancy is the lack of Ca^{2+} store in the model. The Ca^{2+} store was suggested to contribute to the initial transient of the $[Ca^{2+}]_i$ increase as shown in Fig. 4.

The amount of Ca^{2+} flux induced by each physiological mechanism was illustrated separately to examine each mechanism's contribution to the control of $[Ca^{2+}]_i$ (Fig. 8*B*). In this figure, the vertical axis measures the amount of Ca^{2+} extruded

TABLE 2. *Parameter values of the model equations for the voltage-gated K^+ conductances and the passive properties*

Physiological Mechanisms	Estimated Values	Units
Anomalous rectifier K^+ conductance	$E_K = -56.2$	[mV]
	$\overline{g_{anom}} = 2.4$	[mS/cm^2]
	$p_{anom} = 3$	
	$q_{anom} = 0$	
	$\alpha_{m_{anom}} = 0.0951 \cdot \exp((-75 - V_m)/100)$	[1/ms]
	$\beta_{m_{anom}} = \dfrac{0.451}{\exp((-38 - V_m)/10) + 1}$	[1/ms]
Delayed rectifier K^+ conductance	$\overline{g_{K_V}} = 30$	[μS/cm^2]
	$p_{K_V} = 3$	
	$q_{K_V} = 0$	
	$\alpha_{m_{K_V}} = 0.00014 \cdot \dfrac{-34.6 - V_m}{\exp((-34.6 - V_m)/11.5) - 1}$	[1/ms]
	$\beta_{m_KV} = 0.0064 \cdot \exp((-15 - V_m)/10.6)$	[1/ms]
Transient A-type K^+ conductance	$\overline{g_A} = 500$	[μS/cm^2]
	$p_A = 3$	
	$q_A = 2$	
	$\alpha_{m_A} = 0.00037 \cdot \dfrac{-835.5 - V_m}{\exp((-835.5 - V_m)/14.3) - 1}$	[1/ms]
	$\beta_{m_A} = 0.139 \cdot \exp((72.8 - V_m)/45.9)$	[1/ms]
	$\alpha_{h_A} = 0.049 \cdot \exp((-124 - V_m)/16)$	[1/ms]
	$\beta_{h_A} = \dfrac{3.5}{\exp((155 - V_m)/17.5) + 1}$	[1/ms]
Passive leakage conductance	$g_{leak} = 15$	[μS/cm^2]
	$E_{leak} = -57$	[mV]
Membrane capacitance	$c_m = 1.5$	[μF/cm^2]
Cytoplasmic resistance	$r_i = 250$	[$\Omega \cdot$ cm]

See text for details.

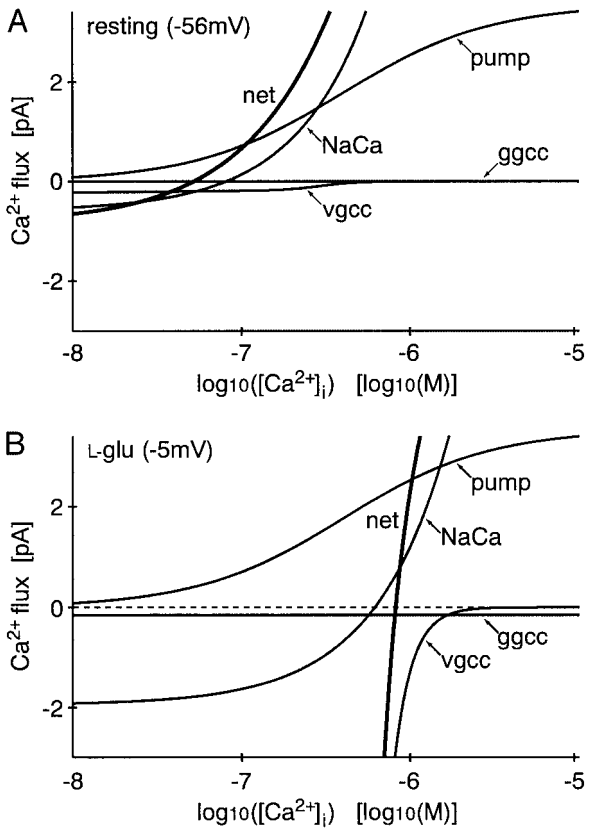

FIG. 6. Relationships between the Ca^{2+} flux and $[Ca^{2+}]_i$ in the steady states. ggcc, vgcc, NaCa and pump indicate the Ca^{2+} flux through the glutamate-gated cation conductance, voltage-gated Ca^{2+} conductance, Na^+/Ca^{2+} exchanger, and Ca^{2+} pump, respectively. The Ca^{2+} flux was calculated with *Eqs. 2* and *3* for ggcc, *Eqs. 4* and *5* for vgcc, *Eq. 6* for NaCa, and *Eq. 7* for pump. The parameters shown in Table 1 were used for the calculations and area of the cell membrane was assumed to be $1.4 \times 10^{-5}cm^2$. net indicates the net flux of Ca^{2+} across the membrane. Upward deflection shows the efflux. *A*: the Ca^{2+} flux was calculated for the resting state in which the membrane voltage is about −56 mV. *B*: the Ca^{2+} flux were calculated for the L-glu-induced depolarized state in which the membrane voltage is about −5 mV.

from the cell. When L-glu is applied, a large influx of Ca^{2+} occurs through the voltage-gated Ca^{2+} conductance that increases $[Ca^{2+}]_i$ to 9.2 μM from 52 nM transiently. The Ca^{2+} efflux mechanisms are activated simultaneously to counteract the influx. At a high $[Ca^{2+}]_i$ seen in the initial phase, Ca^{2+} is extruded mainly by the Na^+/Ca^{2+} exchange because the Ca^{2+} extrusion rate of the Na^+/Ca^{2+} exchange increases monotonically as $[Ca^{2+}]_i$, yet that of the Ca^{2+} pump saturates. The influx of Ca^{2+} through the voltage-gated Ca^{2+} conductance decreases after reaching a peak (−70 pA, *inset*) because of the Ca^{2+}-dependent inactivation. The efflux through the Na^+/Ca^{2+} exchange and the Ca^{2+} pump also decreases as $[Ca^{2+}]_i$ decreases. As a consequence, $[Ca^{2+}]_i$ reaches a steady level of 0.82 μM. These are the fundamental Ca^{2+} regulatory mechanisms of $[Ca^{2+}]_i$ in the isolated horizontal cell during the L-glu application implied by the model.

In the present model, the Ca^{2+} flux by the Na^+/Ca^{2+} exchange is inward in the resting state. The difference of Ca^{2+} regulation properties between the Ca^{2+} pump and the Na^+/Ca^{2+} exchange may suggest the functional difference in regulating $[Ca^{2+}]_i$ between them (DISCUSSION).

When the time constant of Ca^{2+}-dependent inactivation of the voltage-gated Ca^{2+} conductance is removed from *Eq. 5*, the influx through the voltage-gated Ca^{2+} conductance decreases with a faster time course than that shown in the *inset* and a transient increase of $[Ca^{2+}]_i$ does not appear (data not shown). Therefore a part of the falling phase of $[Ca^{2+}]_i$ transient during the L-glu application can be explained by the Ca^{2+}-dependent inactivation of the voltage-gated Ca^{2+} conductance.

Simulation of voltage response to L-glu application

The voltage response to the L-glu application calculated with the cell model was compared with the experimental data as shown in Fig. 9; — shows the calculated membrane potential and ○ show the measured voltage with the perforated-patch electrode. As shown in the figure, the membrane potential of the cell model was depolarized from −56 to −5 mV in response to the L-glu application, which is similar to the experiment. It is notable that the transient overshoot seen in the experiment is well reproduced by the model. As was shown in the previous section, the decline of the overshoot is explained by the Ca^{2+}-dependent inactivation of voltage-gated Ca^{2+} current. Therefore the transient depolarization seen at the initial phase is a Ca^{2+} spike induced by the L-glu application.

DISCUSSION

Computer simulation models of solitary horizontal cells with ionic currents have been previously developed (Usui et al. 1996; Winslow 1989). The biophysical model was developed in the present study based on not only electrophysiological experiments but also optical measurements. Although there are

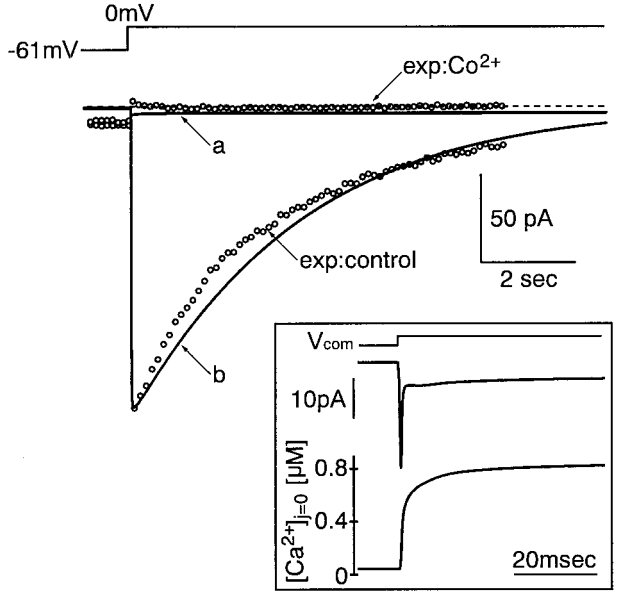

FIG. 7. The time course of Ca^{2+}-dependent inactivation of the voltage-gated Ca^{2+} current. The experimental data were replotted from Fig. 6 of Tachibana (1983) and were illustrated with ○. The membrane voltage of the model was depolarized from −61 to 0 mV to simulate the voltage-clamp experiment. A Co^{2+}-sensitive current, composed of the voltage-gated Ca^{2+} current and the Na^+/Ca^{2+} exchange current, was calculated with the cell model. a and b indicate the Co^{2+}-sensitive current calculated with $\tau_{Ca} = 0$ and $\tau_{Ca} = 2.86$ s, respectively. The other parameters used for the calculations are shown in Table 1. *Inset*: the Co^{2+}-sensitive current and the Ca^{2+} concentration just below the membrane ($[Ca^{2+}]_{j=0}$) calculated with $\tau_{Ca} = 0$ s.

various physiological parameters to be estimated in the model, the ranges of these parameter values were determined by elucidating the results from both electrophysiological and optical measurements. Therefore the present model is physiologically realistic especially in terms of the cooperative activities of the voltage-gated conductances and the Ca^{2+} regulation mechanisms.

The horizontal cell in situ has a membrane potential of around −30 mV and responds to light with a graded potential change. Among the ionic conductances found in the horizontal cell, the voltage-gated Ca^{2+} conductance drastically changes in this voltage range and strongly affects the response of the horizontal cell. The Ca^{2+} conductance is known to be activated around −40 mV and increases prominently until ~0 mV in the horizontal cell of the lower vertebrates (Lasater 1986; Shingai and Christensen 1983, 1986; Tachibana 1983). Therefore a small amount of voltage change produces a significant change in the Ca^{2+} influx. In other outer retinal neurons, i.e., photoreceptors and bipolar cells, the Ca^{2+}-activated K^+ and Ca^{2+}-activated Cl^- currents are thought to counteract the inward Ca^{2+} current to suppress Ca^{2+} spikes (e.g., Bader et al. 1982; Barnes and Hille 1989; Yagi and MacLeish 1994 for photoreceptors; Kaneko and Tachibana 1985; Karschin and Wässle 1990 for bipolar cells). In the horizontal cells, however, such Ca^{2+}-activated outward currents were not observed (Tachibana 1983; Ueda et al. 1992) or too small to suppress the Ca^{2+} spikes (unpublished data). Our previous experiments on isolated horizontal cells have demonstrated that $[Ca^{2+}]_i$ is maintained at a high level and the voltage-gated Ca^{2+} conductance is inactivated to a large extent during the L-glu application (Hayashida et al. 1998) (see also Fig. 2*A*). These suggest that the feed-back control of the voltage-gated Ca^{2+} conductance by the intracellular Ca^{2+} is expected to play an essential role in stabilizing the membrane potential of the horizontal cell in situ. It was suggested that the inactivation of the voltage-gated Ca^{2+} conductance as well as the tonic synaptic input from the photoreceptors are required to account for the membrane potential in the dark and light-induced hyperpolarizing responses of horizontal cells (Winslow 1989). The quantitative analyses in the present study clearly demonstrated the underlying mechanisms to control $[Ca^{2+}]_i$ and the membrane potential.

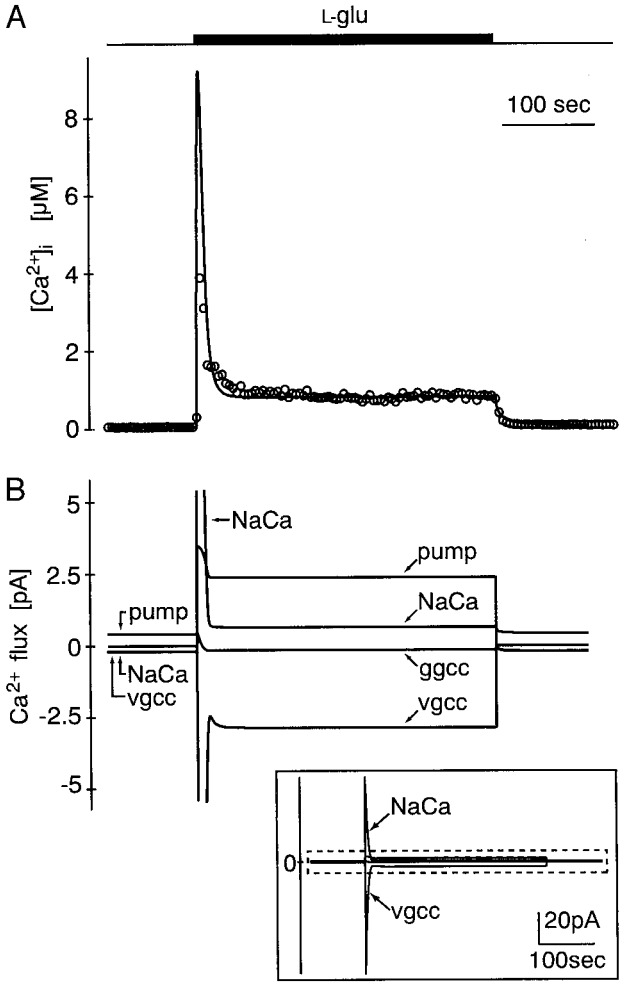

FIG. 8. Simulation of L-glu-induced $[Ca^{2+}]_i$ change using the cable model of isolated horizontal cell. The parameters shown in Tables 1 and 2 were used for the calculations. The glutamate-gated conductance incorporated in the cable surface was calculated with *Eq. 3*, where g_{glu} = 232 mS/cm^2 and τ_{glu} = 100 ms. *A*: the average $[Ca^{2+}]_i$ of the whole cable was calculated (—). ○, the $[Ca^{2+}]_i$ change shown in Fig. 2*A*. *B*: the Ca^{2+} flux through the Ca^{2+} regulation mechanisms was calculated. ggcc, vgcc, NaCa, and pump indicate the Ca^{2+} flux through the glutamate-gated cation conductance, voltage-gated Ca^{2+} conductance, Na^+/Ca^{2+} exchanger, and Ca^{2+} pump, respectively. The traces of Ca^{2+} flux are enlarged from the *inset* (- - -). Upward deflections show the efflux.

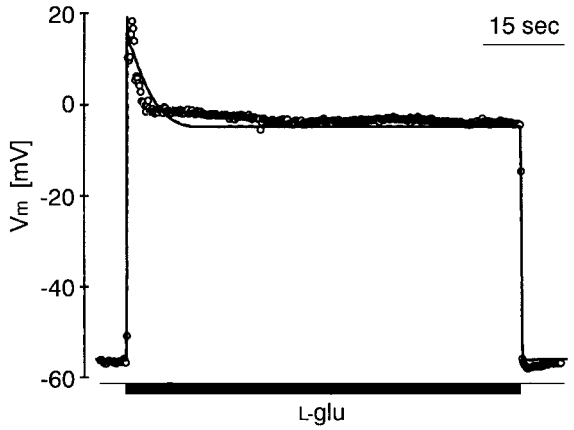

FIG. 9. The voltage response to a L-glu application. The membrane voltage change was calculated with the cable model (—). The parameters shown in Tables 1 and 2 were used for the calculation. The glutamate-gated conductance was calculated with *Eq. 3*, where g_{glu} = 232mS/cm^2 and τ_{glu} = 100 ms. The membrane voltage of the isolated horizontal cell was measured under the current-clamp in the perforated-patch configuration and was shown with ○. L-Glutamate (100 μM) was applied for 74 s.

Previous studies showed that a caffeine-sensitive Ca^{2+} store exists in horizontal cells (Linn and Christensen 1992; Micci and Christensen 1998; Yasui 1988). In the L-glu-induced sustained depolarization as well as the resting state, the Ca^{2+} store is considered to be at steady state and no net release (or uptake) of Ca^{2+} by the store takes place. In the present study, we mainly focused on the regulatory mechanism of $[Ca^{2+}]_i$ in the steady states. Therefore the Ca^{2+} store was not taken into account in the present model.

The preapplication of caffeine suppressed the transient increase of $[Ca^{2+}]_i$ induced by the L-glu application (Fig. 4), suggesting a contribution of the Ca^{2+} store to the transient phase of the L-glu-induced $[Ca^{2+}]_i$ increase in the isolated horizontal cell. The release as well as the uptake of Ca^{2+} by the Ca^{2+} store is likely to occur transiently by an abrupt Ca^{2+}

influx. In the isolated horizontal cell, this abrupt Ca^{2+} influx was induced by a quick application of high concentration of L-glu or by an instantaneous voltage clamp from the resting potential to the potential in which the Ca^{2+} conductance is almost fully activated. This is not considered to be a normal physiological condition in situ. The Ca^{2+} store, however, could contribute to the depolarizing phase after the cell was fully hyperpolarized by bright light.

A possible contribution of the caffeine-sensitive Ca^{2+} store to the inactivation of the L-type Ca^{2+} channel on a long time scale has been demonstrated in rod photoreceptors (Krizaj et al. 1999). The caffeine-sensitive Ca^{2+} store in the horizontal cell might play a functional role in such inactivation of the voltage-gated Ca^{2+} conductance. The effect of caffeine on the L-glu-induced steady $[Ca^{2+}]_i$ level was examined in the isolated horizontal cell. The L-glu-induced $[Ca^{2+}]_i$ level was lowered when caffeine (2–10 mM) was applied to the cell ($n = 5$, data not shown). Further experiments, however, are needed to clarify the role of the Ca^{2+} store in the horizontal cell.

In horizontal cells, both the Na^+/Ca^{2+} exchange and the Ca^{2+} pump operate together (Hayashida et al. 1998). The present simulations indicated that Ca^{2+} was extruded mainly by the Ca^{2+} pump when $[Ca^{2+}]_i$ was lower than 1 μM, but the Na^+/Ca^{2+} exchange became dominant as $[Ca^{2+}]_i$ increased further. These two transporters cooperate to control intracellular Ca^{2+} over a wide range of concentrations. The level of $[Ca^{2+}]_i$, however, might be different at different sites in the horizontal cell in situ. Therefore it is possible that these mechanisms control different cellular functions. The present simulation suggested that the Na^+/Ca^{2+} exchange may operate in the reverse mode when the cell is in the resting state (Fig. 8*B*). This is consistent with the Ca^{2+} influx via the Na^+/Ca^{2+} exchange demonstrated in the isolated catfish horizontal cell (Micci and Christensen 1998). Such a small amount of Ca^{2+} influx in the resting state might play an important role in loading and/or unloading the Ca^{2+} store (Blaustein 1993; Micci and Christensen 1998). Ca^{2+} possibly enters the cell through a leakage conductance. Therefore $[Ca^{2+}]_i$ at the resting state might be maintained by the balance between the efflux through the Ca^{2+} pump and the influx through the reversed Na^+/Ca^{2+} exchange and/or the leakage conductance.

Na^+ continuously enters the cell through the glutamate-gated cation conductance during the application of L-glu (Ishida et al. 1984; Tachibana 1985) and is assumed to be extruded by the Na^+/K^+ pump (Shimura et al. 1998; Yasui 1987, 1988). Therefore $[Na^+]_i$ is likely to be as dynamically changing and controlled as $[Ca^{2+}]_i$. $[Na^+]_i$ affects the regulation of $[Ca^{2+}]_i$ via the Na^+/Ca^{2+} exchange. In the present simulation, $[Na^+]_i$ was assumed to be constant (8 mM) to calculate the Na^+/Ca^{2+} exchange current. The role of the Na^+/K^+ pump as well as the other Na^+ transporters are to be studied further.

The present study revealed fundamental mechanisms to explain Ca^{2+} regulation in the horizontal cell in vitro. Further studies with experimental and computational analyses are needed to elucidate the underlying mechanisms of the light-induced response of the horizontal cell in situ. The model equations of physiological mechanisms developed in the present study are useful, when such studies are conducted.

The authors are grateful to H. Ohno for technical assistance with the computer simulations and to Dr. M. Hines for instructions on the use of NEURON. The authors thank K. H. Sienko for correcting the English of the earlier version of the manuscript and A. T. Ishida for comments on the manuscript.

This work was partially supported by the Japan Society for the Promotion of Science, Grant-in-Aid for Research for the Future Program, JSPS-RFTF 97 I00101 (Principal Investigator: T. Yamakawa of Kyushu Institute of Technology).

REFERENCES

BADER CR, BERTRAND D, AND SCHWARTZ EA. Voltage-activated and calcium-activated currents studied in solitary rod inner segments from the salamander retina. *J Physiol (Lond)* 331: 253–284, 1982.

BARNES S AND HILLE B. Ionic channels of the inner segment of tiger salamander cone photoreceptors. *J Gen Physiol* 94: 719–743, 1989.

BLAUSTEIN MP. Physiological effects of endogenous ouabain: control of intracellular Ca^{2+} stores and cell responsiveness. *Am J Physiol* 264: 1367–1387, 1993.

CERVETTO L, LAGNADO L, PERRY RJ, ROBINSON DW, AND MACNAUGHTON PA. Extrusion of calcium from rod outer segments is driven by both sodium and potassium gradients. *Nature* 337: 740–743, 1989.

CERVETTO L AND MACNICHOL EF. Inactivation of horizontal cells in the turtle retina by glutamate and aspartate. *Science* 178: 767–768, 1972.

DOWLING JE AND RIPPS H. Adaptation in skate photoreceptors. *J Gen Physiol* 60: 698–719, 1972.

EHLERS MD AND AUGUSTINE GJ. Calmodulin at the channel gate. *Nature* 399: 105–108, 1999.

GRYNKIEWICZ G, POENIE M, AND TSIEN RY. A new generation of Ca^{2+} indicators with greatly improved fluorescence properties. *J Biol Chem* 260: 3440–3450, 1985.

HAYASHIDA Y, YAGI T, AND YASUI S. Ca^{2+} regulation by the Na^+-Ca^{2+} exchanger in retinal horizontal cells depolarized by L-glutamate. *Neurosci Res* 31: 189–199, 1998.

HINES ML AND CARNEVALE NT. The NEURON simulation environment. *Neural Comput* 9: 1179–1209, 1997.

HINES ML AND CARNEVALE NT. Expanding NEURON′s. Repertoire of mechanisms with NMODL. *Neural Comput* 12: 995–1007, 2000.

HORN R AND MARTY A. Muscarinic activation of ionic currents measured by a new whole-cell recording method. *J Gen Physiol* 92: 145–159, 1988.

ISHIDA AT, KANEKO A, AND TACHIBANA M. Responses of solitary retinal horizontal cells from *Carassius auratus* to L-glutamate and related amino acids. *J Physiol (Lond)* 348: 255–270, 1984.

ISHIDA AT AND NEYTON J. Quisqualate and L-glutamate inhibit retinal horizontal-cell responses to kainate. *Proc Natl Acad Sci USA* 82: 1837–1841, 1985.

JONAS P AND BURNASHEV N. Molecular mechanisms controlling calcium entry through AMPA-type glutamate receptor channels. *Neuron* 15: 987–990, 1995.

KANEKO A. The functional role of retinal horizontal cells. *Jpn J Physiol* 37: 341–358, 1987.

KANEKO A AND TACHIBANA M. A voltage-clamp analysis of membrane currents in solitary bipolar cells dissociated from Carassius auratus. *J Physiol (Lond)* 358: 131–152, 1985.

KARSCHIN A AND WÄSSLE H. Voltage- and transmitter-gated currents in isolated rod bipolar cells of rat retina. *J Neurophysiol* 63: 860–876, 1990.

KRIZAJ D, BAO J-X, SCHMITZ Y, WITKOVSKY P, AND COPENHAGEN DR. Caffeine-sensitive calcium stores regulate synaptic transmission from retinal rod photoreceptors. *J Neurosci* 19: 7249–7261, 1999.

KUSHMERICK MJ AND PODOLSKY RJ. Ionic mobility in muscle cells. *Science* 166: 1297–1298, 1969.

LASATER EM. Ionic currents of cultured horizontal cells isolated from white perch retina. *J Neurophysiol* 55: 499–513, 1986.

LASATER EM. *Retinal Research.* Oxford: Pergamon, 1991, vol. 11.

LASATER EM AND DOWLING JE. Carp horizontal cells in culture respond selectively to L-glutamate and its agonists. *Proc Natl Acad Sci USA* 79: 936–940, 1982.

LEE S-H, SCHWALLER B, AND NEHER E. Kinetics of Ca^{2+} binding to parvalbumin in bovine chromaffin cells: implications for $[Ca^{2+}]$ transients of neuronal dendrites. *J Physiol (Lond)* 525: 419–432, 2000.

LINN CP AND CHRISTENSEN BN. Excitatory amino acid regulation of intracellular Ca^{2+} in isolated catfish cone horizontal cells measured under voltage- and concentration-clamp conditions. *J Neurosci* 12: 2156–2164, 1992.

MICCI MA AND CHRISTENSEN BN. Na^+/Ca^{2+} exchanger in catfish retinal horizontal cells: regulation of intracellular Ca^{2+} store function. *Am J Physiol* 274: 1625–1633, 1998.

MURAKAMI M, OHTSU K, AND OHTSUKA T. Effects of chemicals on receptors and horizontal cells in the retina. *J Physiol (Lond)* 227: 899–913, 1972.

MURAKAMI M AND TAKAHASHI K. Calcium action potential and its use for measurement of reversal potentials of horizontal cell responses in carp retina. *J Physiol (Lond)* 386: 165–180, 1987.

O'DELL T AND CHRISTENSEN BN. N-methyl-D-aspartate receptors coexist with kainate and quisqualate receptors on single isolated catfish horizontal cells. *Brain Res* 381: 359–362, 1986.

O'DELL TJ AND CHRISTENSEN BN. Horizontal cells isolated from catfish retina contain two types of excitatory amino acid receptors. *J Neurophysiol* 61: 1097–1109, 1989.

OKADA T, SCHULTZ K, GEURTZ W, HATT H, AND WEILER R. AMPA-preferring receptors with high Ca^{2+} permeability mediate dendritic plasticity of retinal horizontal cells. *Eur J Neurosci* 11: 1085–1095, 1999.

PICAUD S, HICKS D, FORSTER V, SAHEL J, AND DREYFUS H. Adult human retinal neurons in culture: physiology of horizontal cells. *Invest Ophthalmol Vis Sci* 39: 2637–2648, 1998.

SHIMURA M, TAMAI M, ZUSHI I, AND AKAIKE N. Characterization of the electrogenic Na^+-K^+ pump in horizontal cells isolated from the carp retina. *Neuroscience* 86: 233–240, 1998.

SHINGAI R AND CHRISTENSEN BN. Sodium and calcium currents measured in isolated catfish horizontal cells under voltage clamp. *Neuroscience* 10: 893–897, 1983.

SHINGAI R AND CHRISTENSEN BN. Excitable properties and voltage-sensitive ion conductances of horizontal cells isolated from catfish (*Ictalurus punctatus*) retina. *J Neurophysiol* 56: 32–49, 1986.

SULLIVAN JM AND LASATER EM. Sustained and transient calcium currents in horizontal cells of the white bass retina. *J Gen Physiol* 99: 84–107, 1992.

SUZUKI S, TACHIBANA M, AND KANEKO A. Effects of glycine and GABA on isolated bipolar cells of the mouse retina. *J Physiol (Lond)* 421: 645–662, 1990.

TACHIBANA M. Membrane properties of solitary horizontal cells isolated from goldfish retina. *J Physiol (Lond)* 321: 141–161, 1981.

TACHIBANA M. Ionic currents of solitary horizontal cells isolated from goldfish retina. *J Physiol (Lond)* 345: 329–351, 1983.

TACHIBANA M. Permeability changes induced by L-glutamate in solitary retinal horizontal cells isolated from *Carassius auratus*. *J Physiol (Lond)* 358: 153–167, 1985.

UEDA Y, KANEKO A, AND KANEDA M. Voltage-dependent ionic currents in solitary horizontal cells isolated from cat retina. *J Neurophysiol* 68: 1143–1150, 1992.

USUI S, KAMIYAMA Y, ISHII H, AND IKENO H. Reconstruction of retinal horizontal cell responses by the ionic current model. *Vision Res* 36: 1711–1719, 1996.

VONGERSDORFF H AND MATTHEWS G. Calcium-dependent inactivation of calcium current in synaptic terminals of retinal bipolar neurons. *J Neurosci* 16: 115–122, 1996.

WINSLOW RL. Bifurcation analysis of nonlinear retinal horizontal cell models. I. Properties of isolated cells. *J Neurophysiol* 62: 738–749, 1989.

YAGI T. Dynamics of signal conduction from soma to axon terminal of the teleost retinal horizontal cell: *in vivo*, *in vitro* and model studies. *Vision Res* 29: 375–384, 1989.

YAGI T AND KANEKO A. The axon terminal of goldfish retinal horizontal cells: a low membrane conductance measured in solitary preparations and its implication to the signal conduction from the soma. *J Neurophysiol* 59: 482–494, 1988.

YAGI T AND MACLEISH PR. Ionic conductances of monkey solitary cone inner segments. *J Neurophysiol* 71: 656–665, 1994.

YASUI S. Ca and Na homeostasis in horizontal cells of the cyprinid fish retina: evidence for Na-Ca exchanger and Na-K pump. *Neurosci Res Suppl* 6: 133–146, 1987.

YASUI S. Na-Ca exchanger, Na-K ATPase and calcium stores in retinal horizontal cells. *Biomed Res* 9: 119–123, 1988.

ZADOR A, KOCH C, AND BROWN TH. Biophysical model of a Hebbian synapse. *Proc Natl Acad Sci USA* 87: 6718–6722, 1990.